Cell Host & Microbe
Article

Caspase-1 Cleavage of the TLR Adaptor TRIF Inhibits Autophagy and β-Interferon Production during *Pseudomonas aeruginosa* Infection

Majid Sakhi Jabir,[1,2] Neil D. Ritchie,[1] Dong Li,[1] Hannah K. Bayes,[1] Panagiotis Tourlomousis,[3] Daniel Puleston,[4] Alison Lupton,[5] Lee Hopkins,[3] Anna Katharina Simon,[4] Clare Bryant,[3] and Thomas J. Evans[1,*]
[1]Institute of Immunity, Infection and Inflammation, University of Glasgow, Glasgow G12 8TA, UK
[2]University of Technology, Applied Science School, Biotechnology Department, Baghdad, Iraq
[3]Department of Veterinary Medicine, University of Cambridge, Cambridge, CB3 0ES UK
[4]Human Immunology Unit, Weatherall Institute of Molecular Medicine, University of Oxford, Oxford, OX3 9DS, UK
[5]Department of Pathology, Western Infirmary, Glasgow G11 6NT, UK
*Correspondence: tom.evans@glasgow.ac.uk
http://dx.doi.org/10.1016/j.chom.2014.01.010

SUMMARY

Bacterial infection can trigger autophagy and inflammasome activation, but the effects of inflammasome activation on autophagy are unknown. We examined this in the context of *Pseudomonas aeruginosa* macrophage infection, which triggers NLRC4 inflammasome activation. *P. aeruginosa* induced autophagy via TLR4 and its adaptor TRIF. NLRC4 and caspase-1 activation following infection attenuated autophagy. Caspase-1 directly cleaved TRIF to diminish TRIF-mediated signaling, resulting in inhibition of autophagy and in reduced type I interferon production. Expression of a caspase-1 resistant TRIF mutant enhanced autophagy and type I interferon production following infection. Preventing TRIF cleavage by caspase-1 in an in vivo model of *P. aeruginosa* infection resulted in enhanced bacterial autophagy, attenuated IL-1β production, and increased bacterial clearance. Additionally, TRIF cleavage by caspase-1 diminished NLRP3 inflammasome activation. Thus, caspase-1 mediated TRIF cleavage is a key event in controlling autophagy, type I interferon production, and inflammasome activation with important functional consequences.

INTRODUCTION

Microbial interactions with host immune cells can trigger macroautophagy (Deretic and Levine, 2009; Orvedahl and Levine, 2009) (hereafter termed autophagy) and activation of the inflammasome (Franchi et al., 2012b; Martinon et al., 2009). Autophagy is important in host defense against a number of microbes (Deretic and Levine, 2009). The inflammasome is a multisubunit platform for the activation of caspase-1, resulting in processing of IL-1β and IL-18 from inactive precursors to their active secreted forms (Franchi et al., 2009; Martinon et al., 2009; Yu and Finlay, 2008). It also triggers a form of cell death termed pyroptosis, itself also important in host defense (Miao et al., 2011). Although autophagy and inflammasome activation both play significant roles in host defense against microbial infection, they do have some clear opposing effects. Thus, autophagy can promote cell survival (Baehrecke, 2005) while inflammasome activation will lead to cell death by pyroptosis (Bergsbaken et al., 2009). Additionally, autophagy can act to downregulate inflammasome activation by the sequestration of defective mitochondria (mitophagy) (Saitoh et al., 2008). This results in inhibiting the release of mitochondrial reactive oxygen intermediates and mitochondrial DNA that can activate the NLRP3 inflammasome (Martinon, 2012; Nakahira et al., 2011; Shimada et al., 2012). The effects of inflammasome activation on autophagy are not known.

We hypothesized that inflammasome activation would lead to a reciprocal inhibition of autophagy. To test this hypothesis, we used a model system of infection of macrophages with the Gram-negative pathogen *P. aeruginosa,* which activates the NLRC4 inflammasome through a type III secretion system (T3SS)-dependent pathway (Franchi et al., 2007; Miao et al., 2008; Sutterwala et al., 2007). We demonstrate here that *P. aeruginosa* activates autophagy in macrophages following infection and that inhibition of inflammasome and caspase-1 activation augments the autophagocytic response. This inhibitory effect of caspase-1 on induction of autophagy results from caspase-1-mediated cleavage of the signaling intermediate TRIF, an essential part of the TLR4-mediated signaling pathway leading to promotion of autophagy (Xu et al., 2007). Caspase-1 cleavage of TRIF reduced the signaling required to induce type I interferons (IFNs) and attenuated macrophage phagocytosis and reactive oxygen generation. Additionally, the caspase-1-mediated downregulation of autophagy resulted in a reduction of NLRP3 inflammasome activation by LPS + ATP.

RESULTS

P. aeruginosa Induces Autophagy that Is Enhanced in the Absence of a Functional T3SS

P. aeruginosa PAO1 has been shown to induce autophagy (Yuan et al., 2012). We set out to determine the influence of the T3SS upon this process. We used a strain of *P. aeruginosa*, PA103ΔUΔT, that has a functional T3SS but does not translocate

any exotoxins and an isogenic strain, PA103pcrV^{-}, that lacks a functional T3SS (Frank et al., 2002; Vallis et al., 1999). To quantify autophagy, we followed the conversion of the protein microtubule-associated protein 1 light chain 3 beta (LC3) to its lipidated form (LC3 II) by western blot (Figure 1A) (Mizushima et al., 2010). This clearly demonstrated a marked increase in the absolute amount of LC3 II relative to β-tubulin following infection that was significantly greater following infection with a *P. aeruginosa* isogenic strain that lacked PcrV (Figures 1A and 1B). Specificity of the immunoblot staining was additionally confirmed by knockdown of *Lc3b* RNA using siRNA (Figure 1A).

We confirmed that the increase in LC3 II reflected an increase in flux through the autophagocytic pathway by repeating the experiment in the presence of inhibitors of lysosomal degradation (Figure S1A available online). These increased still further the amounts of LC3 II following infection, showing that the increased levels observed were due to greater flux of LC3 through the autophagocytic pathway and not by inhibition of LC3 processing. To confirm these observations, we determined the localization of endogenous LC3 to autophagocytic vacuoles using immunofluorescence. Following infection with *P. aeruginosa*, we observed a marked increase in the number of LC3-containing vacuoles within bone-marrow-derived macrophages (BMDMs), which were consistently significantly higher in the T3SS defective mutant (Figures 1C and 1D), and to a level comparable to that seen with rapamycin. We quantified changes in *Lc3b* expression using RT-PCR (Figure S1B). *P. aeruginosa* infection increased the expression of *Lc3b* as has been described in the induction of autophagy in other systems, notably yeast (Stromhaug and Klionsky, 2001). The increase in *Lc3b* expression was higher in the T3SS mutant, consistent with the results obtained by western blotting and immunofluorescence.

Finally, we used a validated flow cytometric method to quantify intracellular LC3 II staining following cell permeabilization (Figure S1C). This also showed that the level of autophagy was increased in the absence of a functional T3SS. Transmission electron microscopy confirmed the presence of autophagosomes containing cytoplasmic contents (Figure 1E). In these panels, the double membrane structure of the autophagosome is arrowed and surrounds another membrane-bound organelle, probably a degraded mitochondrion as well as other cytoplasmic structures. Importantly, under the conditions of these experiments, we did not observe a significant increase in cell death, as measured by the release of LDH (Figure 1F). We tested the dependence of autophagy following *P. aeruginosa* infection on the genes *Atg7* and *Atg5*. Infection of BMDMs lacking these gene products showed a marked reduction in autophagy (Figures 1G–1I, S1D, and S1E).

Caspase-1 Activation by the Inflammasome Downregulates Autophagy

The reduction in autophagy following infection with *P. aeruginosa* in a strain with a functional T3SS suggested that this might be due to the effects of caspase-1 activation by the inflammasome that is induced by the T3SS. We thus tested the effect of a selective caspase-1 inhibitor on autophagy following PA103ΔUΔT infection; this drug produced the expected reduction in caspase-1 processing and secretion of IL-1β (Figures S2A and S2B) while enhancing autophagy (Figures 2A and 2B). Infection of BMDMs lacking *Capsase-1* showed increased autophagy (Figure 2C). However, these *Casp1*$^{-/-}$ animals also lack a functional Caspase-11, also important in inflammasome activation (Kayagaki et al., 2011; Rathinam et al., 2012). We tested specifically for a role of Caspase-1 by knocking down the gene using siRNA (Figure 2D), which resulted in increased autophagy (Figures 2E–2G). Knockdown of Caspase-11 (Figure 2H) had no effect on induction of autophagy or production of IL-1β following infection (Figures 2I–2K). Thus, casapse-1 inhibits the process of autophagy following infection with *P. aeruginosa*, but caspase-11 is not involved.

BMDMs from *Nlrc4*$^{-/-}$ animals showed increased autophagy following infection (Figure 2L) with complete loss of production of secreted IL-1β (Figure S2D). Elevation of extracellular K^+ inhibits NLRC4 inflammasome activation by *P. aeruginosa* (Arlehamn et al., 2010). We confirmed that BMDMs incubated in a high extracellular concentration of K^+ had a markedly attenuated production of caspase-1 p10 and IL-1β following infection while maintaining very similar levels of production of TNF-α (Figures S2E–S2G). This inhibitory effect on inflammasome activation resulted in increased autophagy (Figures S2H–S2K). To ensure that elevation of extracellular K^+ did not affect the function of the T3SS, we tested the effects of raising K^+ on a strain expressing only the highly cytotoxic exotoxin ExoU, PA103ΔUΔT:ExoU. In contrast to the parent strain PA103ΔUΔT, the presence of ExoU induces rapid cytotoxicity; this was unaffected by raising extracellular K^+ (Figure S2L). Thus, activation of the NLRC4 inflammasome following *P. aeruginosa* infection leads to an inhibition of autophagy, and this is directly mediated by Caspase-1.

Autophagy following *P. aeruginosa* Infection Is Mediated via TLR4 and TRIF

LPS induces autophagy through TLR4 signaling via TRIF (Xu et al., 2007); we hypothesized that a similar pathway might operate following *P. aeruginosa* infection. We confirmed that LPS induced autophagy in BMDMs (Figure 3A); this was significantly abrogated in BMDMs from *Tlr4* knockout (KO) mice (Figures 3A–3D). Autophagy induced by rapamycin was, as expected, not diminished in the absence of TLR4 (Figure 3B).

We then determined the role of Myd88 and TRIF in the induction of autophagy following *P. aeruginosa* infection. In the absence of *Myd88*, there was no reduction in autophagy following infection (Figure 3E). In macrophages lacking *Trif*, we found that autophagy was greatly reduced (Figures 3F–3H). Thus, *P. aeruginosa* induces autophagy via signaling through TLR4 and the intermediate TRIF.

Caspase-1 Cleaves TRIF

We hypothesized that one mechanism that could explain why caspase-1 activation downregulated autophagy was through proteolytic cleavage of TRIF. To test this hypothesis, we examined cell lysates for endogenous TRIF fragments following infection of BMDMs with *P. aeruginosa* (Figure 4A). After infection with the inflammasome-activating strain PA103ΔUΔT, we observed immunoreactive TRIF fragments between 28 and 30 kDa at 4 hr after infection (Figure 4A). These were not seen following infection with the T3SS inactive strain PA103pcrV^{-} and were also considerably reduced in the presence of a

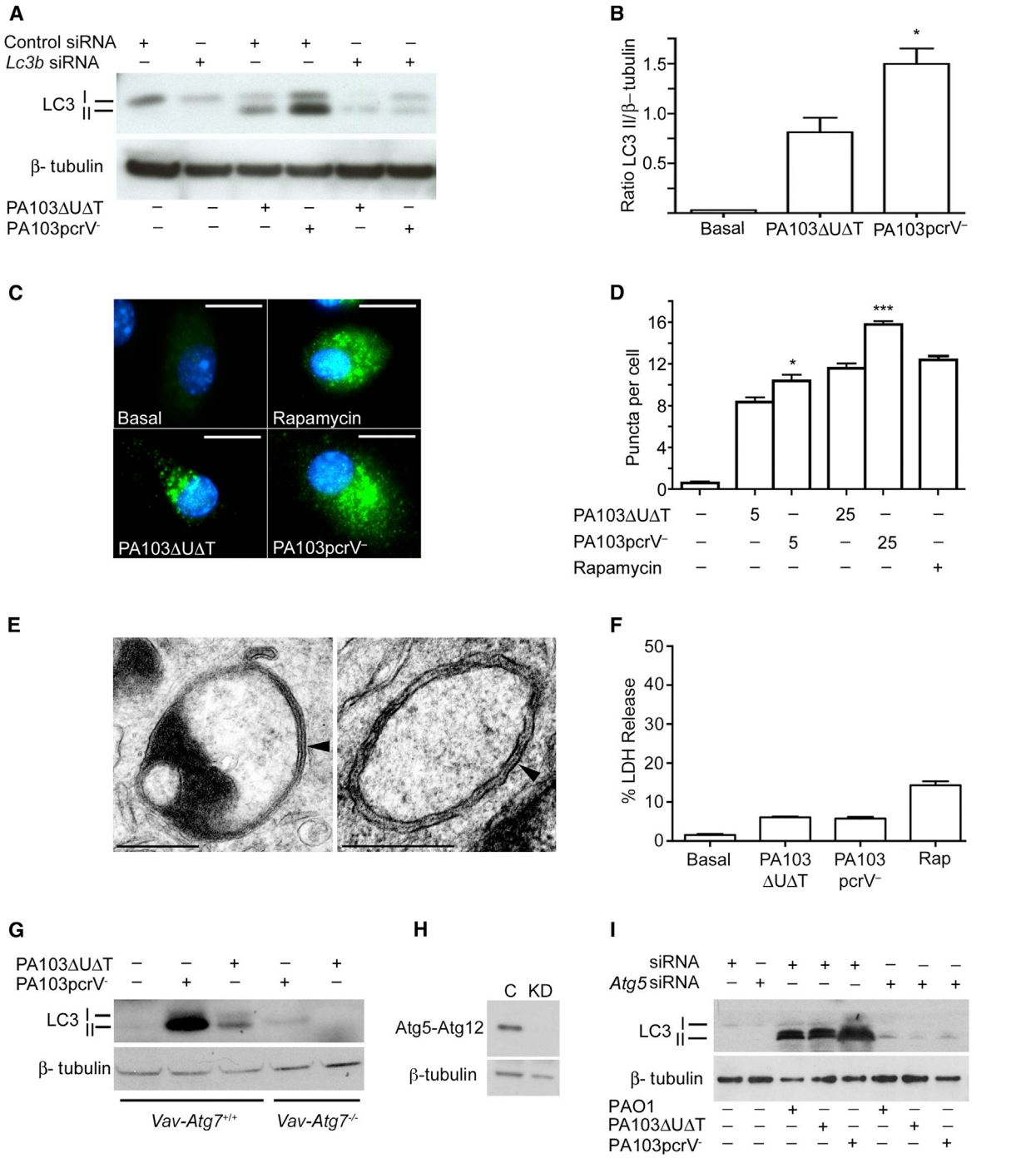

Figure 1. *P. aeruginosa* Induces Autophagy in BMDMs that Is Enhanced in the Absence of a Functional T3SS

(A) Western blot of LC3-I and LC3-II in BMDM treated with control or *Lc3b* siRNA and infected with the indicated strains of *P. aeruginosa* for 4 hr (MOI 25). β-tubulin is shown as loading control (repeated in three independent experiments).

(B) Ratio of LC3-II/β-tubulin in three independent experiments. BMDMs were infected as indicated for 3 hr at a multiplicity of infection (MOI) of 10. Columns are means; error bar SEM. The symbol * indicates statistically different from PA103ΔUΔT; $p < 0.05$.

(C) Representative immunofluorescence images of LC3 in BMDM left uninfected (Basal), treated with rapamycin, or infected with the indicated strains for 4 hr at an MOI of 25. LC3 staining is shown as green and nuclei blue. Scale bar indicates 10 μm (five independent experiments).

(D) Number of LC3 puncta in BMDM cells following infection (at specified MOI) or rapamycin treatment as indicated. Columns are means of triplicates; error bar SEM. Asterisks indicate statistically different from PA103ΔUΔT at the same MOI; *$p < 0.05$; ***$p < 0.001$.

(E) Electron micrographs of autophagosomes in BMDM infected with PA103ΔUΔT (left) or PA103pcrV⁻ (for the right, 4 hr and MOI of 25 for both). Arrows indicate autophagosomes.

(legend continued on next page)

caspase-1 inhibitor (Figure 4A). The antibody used in these immunoblots recognizes a C-terminal epitope, thus suggesting that the cleavage site lies in the middle portion of TRIF (molecular weight 74 kDa) to generate the ~30kDa fragments seen in Figure 4.

To confirm that these cleavage products were produced by caspase-1, we examined lysates from BMDMs from mice lacking the *Caspase-1* gene as well as WT animals (Figure 4B). This showed that the cleavage products were absent following infection of BMDMs lacking *Capsase-1*. We obtained the same results with knockdown of *Caspase-1* (data not shown). Knockdown of caspase-11 had no effect on TRIF cleavage following infection (Figure 4C), which was also seen with the wild-type (WT) PAO1 strain. In macrophages from NLRC4 knockout mice, no TRIF cleavage was seen, either with PA103ΔUΔT or the WT PAO1 (Figure 4D). Similarly, infection of BMDMs in high extracellular potassium (which inhibits inflammasome activation) also inhibited TRIF cleavage (Figure 4E).

To prove that caspase-1 directly cleaved TRIF, we purified recombinant TRIF expressed in HEK cells with the FLAG epitope tag. The previous report that suggested TRIF was a substrate for caspase cleavage identified the aspartic acid residues at positions 281 (VAPDA) and 289 (GLPDT) of the human sequence as essential for caspase-mediated cleavage (Rebsamen et al., 2008). Mutation of both of these residues to glutamic acid residues (D281E D289E) effectively abolished caspase cleavage. Murine TRIF has similar well-conserved caspase-1 cleavage sites at positions 286 (ILPDA) and 292 (AAPDT). We thus additionally purified recombinant FLAG-tagged D281E D289E TRIF from HEK cells. The purified proteins were then incubated with recombinant activated human caspase-1. This cleaved the WT TRIF but not the D281E D289E mutant. Thus, caspase-1 directly cleaves TRIF (Figure 4F).

Prevention of TRIF Cleavage by Capsase-1 Augments Autophagy

To confirm that the cleavage products we observed in Figure 4 were truly derived from TRIF, we expressed FLAG-tagged human TRIF within BMDMs. Following infection with PA103ΔUΔT, we again saw the appearance of a cleaved product of molecular weight ~30kDa (Figure 5A). This was not seen following infection with the T3SS-defective mutant strain PA103pcrV^{-}, which does not activate the inflammasome (Figure 5A). Moreover, mutation of the sites previously identified as essential to TRIF cleavage by caspases also inhibited the production of the cleaved products following infection (cells transfected with plasmid expressing D281E D289E TRIF-FLAG, Figure 5A). The same cleavage of TRIF following infection was observed in human THP-1 cells (Figure 5B).

We hypothesized that cleavage of TRIF would generate products that could exert a dominant negative effect and thus inhibit TRIF function as previously described (Yamamoto et al., 2002). To test this hypothesis, we cloned the segments of TRIF encoding the N-terminal and C-terminal fragments that are generated by caspase-1 cleavage and expressed these in BMDMs. Expression of both the N- and C-terminal fragments individually and together potently inhibited the induction of autophagy following infection (Figure 5C)—even at low levels of expression. The two fragments also inhibited the induction of *Ifnb* mRNA induction in BMDMs following treatment with the TLR3 agonist polyIC (Figure 5D). Thus, caspase-1 cleavage of TRIF generates products that inhibit TRIF induction of autophagy and *Ifnb* gene expression.

Since TRIF is an essential intermediate in initiating autophagy following *P. aeruginosa* infection, prevention of its cleavage by caspase-1 should lead to increased autophagy. We tested this directly by infecting BMDMs transfected with either WT TRIF or the noncleavable D281E D289E TRIF construct. When cells were transfected with the D281E D289E TRIF construct, we observed an increase in the degree of autophagy (Figures 5E–5I). This was under conditions where the expression level of the different TRIF proteins was identical (Figure 5A). Previous study of the TRIF fragments generated by caspase cleavage clearly demonstrated that the D281E D289E mutant TRIF had completely normal signal-transducing functions (Rebsamen et al., 2008). We tested the effects of expression of the D281E D289E mutant TRIF on *Ifnb* expression induced by PolyI:C (Figure S3). Expression of the mutant did not affect TLR3 signal transduction; additionally, no cleavage of TRIF was seen in response to PolyI:C, which does not activate the inflammasome when added extracellularly (Rajan et al., 2010). Thus, the effects of the mutant noncleavable TRIF are not due to effects on overall TRIF function.

Functional Effects of TRIF Inactivation by Capsase-1 in BMDMs

TRIF is required for type I IFN induction following TLR4 activation. We confirmed that in macrophages from mice lacking *Trif*, type I IFN following *P. aeruginosa* infection was abolished (Figure S4A). Blocking caspase-1 activation increased the induction of *Ifnb1* mRNA following infection (Figures S4B and S4C). Similarly, in macrophages from mice lacking *Nlrc4*, infection also resulted in increased type I IFN induction, as expected because of the lack of TRIF cleavage in the absence of NLRC4 (Figure 4D). Blocking inflammasome activation by incubation in media with elevated K^{+} also led to greater *Ifnb1* mRNA induction following infection (Figure S4E). Prevention of TRIF cleavage by transfection of the D281E D289E mutant TRIF also resulted in increased *Ifnb1* mRNA induction following infection (Figure S4F). These data are all consistent with the NLRC4 inflammasome negatively regulating TRIF-dependent type I IFN responses following infection with *P. aeruginosa*.

Next, we determined whether the reduction in type I IFN induction resulting from caspase-1 cleavage of TRIF had functional effects. First, we compared phagocytosis and production of

(F) LDH release caused by *P. aeruginosa* infection in BMDM (4 hr at MOI of 5) or rapamycin treatment. Columns are means of triplicates; error bars are SEM. Differences are not significant. Repeated three times.
(G) LC3 I and II levels in WT BMDMs and those lacking *Atg7* (*Vav-Atg*$^{-/-}$) infected as in (A).
(H) Western blot of Atg-Atg12 conjugate following knockdown (KD) of *Atg5* mRNA. (C) is control siRNA.
(I) Effects of knockdown of *Atg5* on LC3 II levels following infection as in (A) with indicated strains of *P. aeruginosa*. See also Figure S1.

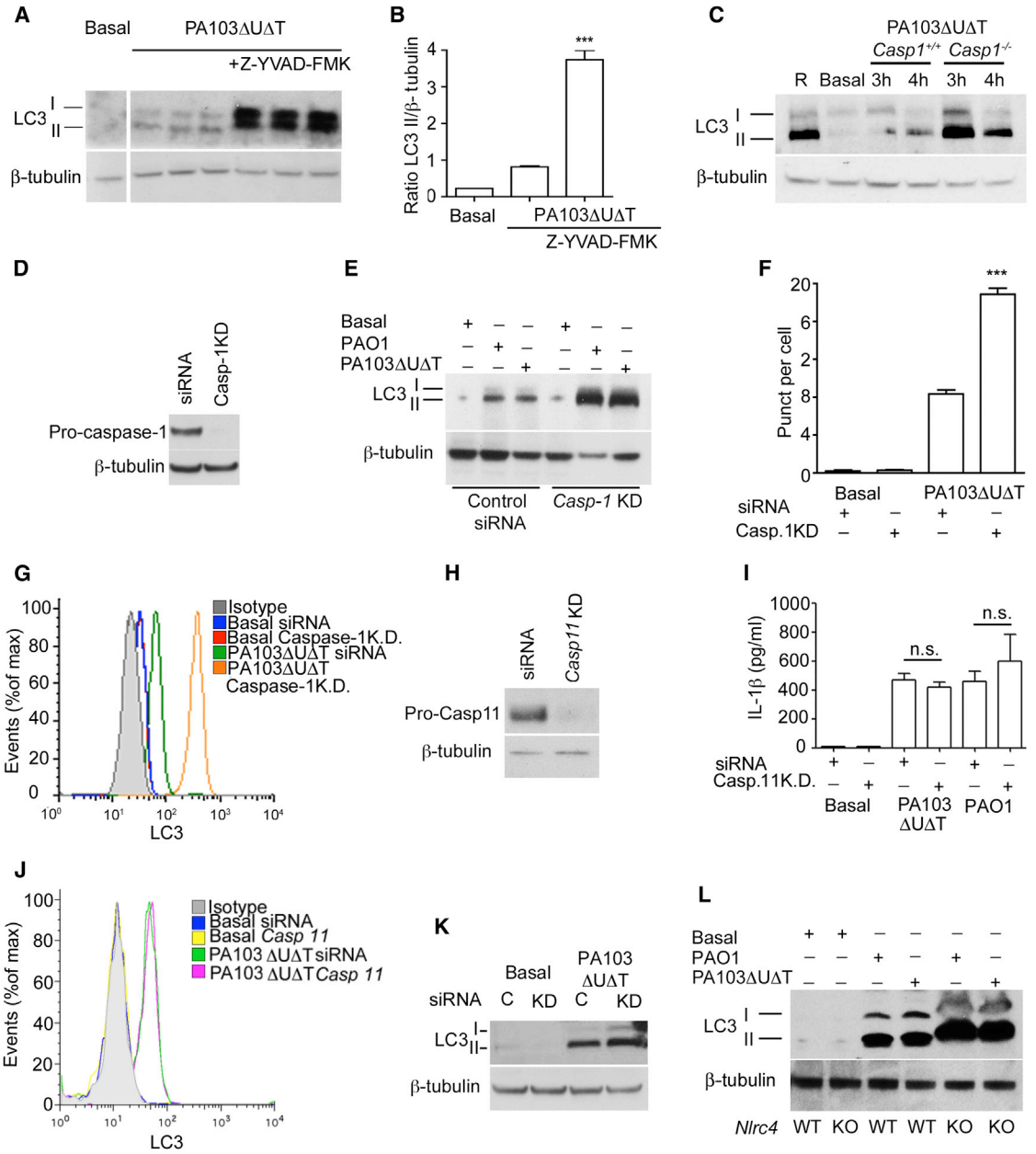

Figure 2. Caspase-1 Downregulates Autophagy

(A and B) Western blot and quantification of LC3 as Figures 1A and 1B in presence and absence of the caspase-1 inhibitor. Five independent experiments; the symbol *** indicates significantly different between untreated and treated cells; $p < 0.001$.

(C) LC3 I and II isoforms in uninfected cells (Basal), treated with rapamycin (R) or infected with PA103ΔUΔT (MOI 25) for the indicated time in hours in WT (*Casp1*$^{+/+}$) or *Casp1*$^{-/-}$ mice. Experiment repeated with the same results.

(D) Western blot of pro-caspase-1 in BMDMs treated with control siRNA or siRNA specific for caspase-1 (+). Levels of β-tubulin are shown as loading control.

(E) LC3 I and II levels following infection for 4 hr at MOI of 25 with strains as shown in BMDMs transfected with control siRNA (C) or siRNA specific for caspase-1 (+).

(F) Number of LC3 puncta per cell with indicated treatments for three independent experiments. Bars are means; error bars are SEM. The symbol ** indicates significantly different from control siRNA; $p < 0.01$.

(G) As (F), but showing intracellular LC3 II after the indicated treatments.

(H) Western blot of Caspase-11 in BMDMs transfected with Control siRNA or siRNA specific for *Casp11*, as indicated; β-tubulin is shown as loading control.

(I) Levels of IL-1β secreted from BMDMs with treatments and infection as indicated.

(J) Assay of intracellular LC3 II after the indicated treatments.

(K) Levels of LC3 I and II in BMDMs either transfected with Control siRNA (C) or siRNA specific to *Casp11* (+) and then left uninfected (basal) or infected, as shown. Experiments in (J) and (K) repeated twice.

(L) LC3 western blot in BMDMs from WT mice (*Nlrc4*$^{+/+}$) or *Nlrc4* knockout animals (*Nlrc4*$^{-/-}$) infected as shown. Experiment repeated with the same result. See also Figure S2.

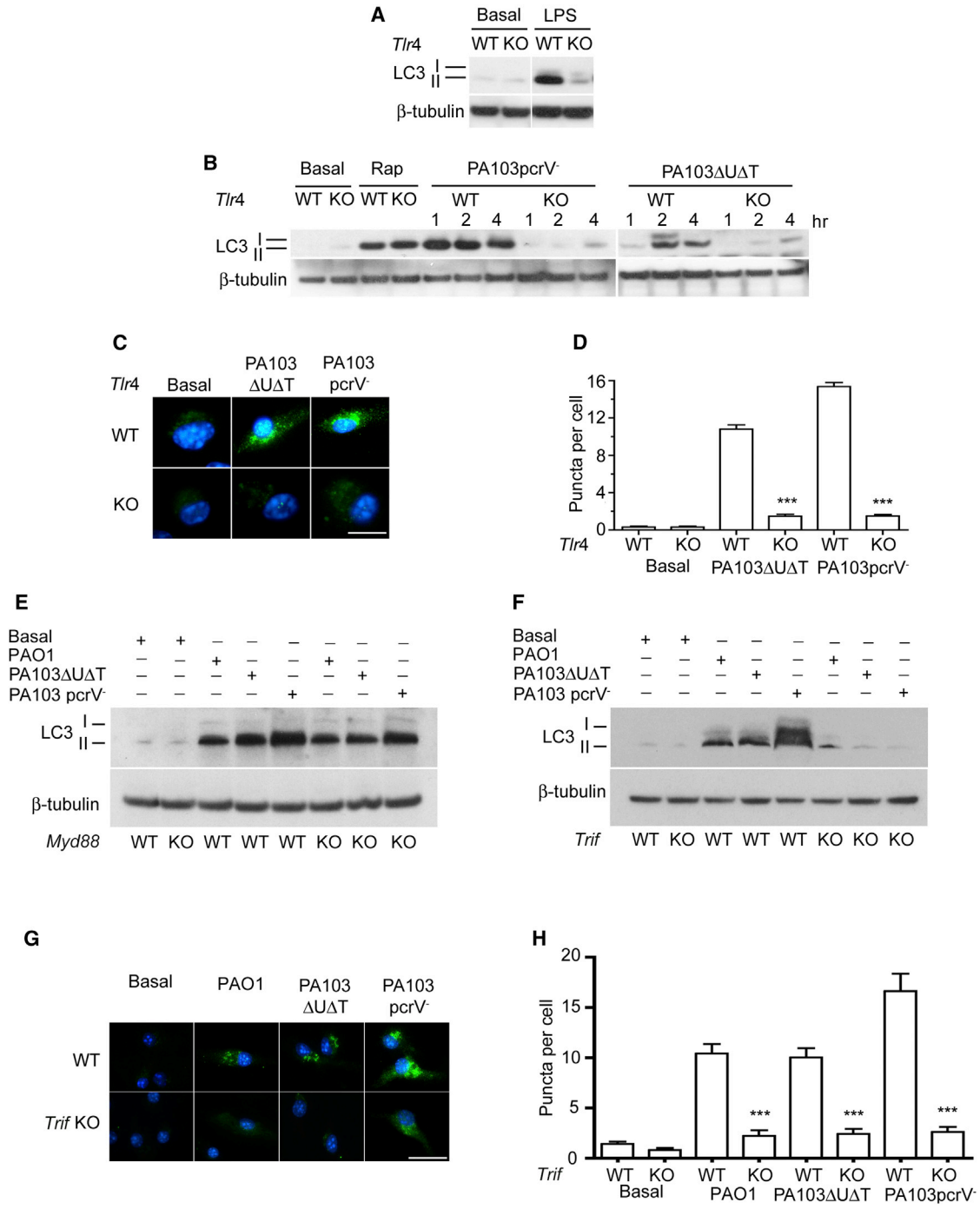

Figure 3. Autophagy following Infection with *P. aeruginosa* Is Dependent on Signaling through TLR4 and TRIF

(A and B) LC3 I and II in BMDMs from WT or *Tlr4*$^{-/-}$ mice (KO), uninfected (Basal), treated with LPS, rapamycin (Rap), or infected with *P. aeruginosa* strains as indicated (MOI 25). Experiment repeated on two occasions with same results.

(C) Representative immunofluorescence images of LC3 staining (green) in BMDMs treated by the strains as indicated under the same conditions as in Figure 1C. Scale bar is 10 μm.

(D) Number of puncta per cell in BMDMs infected as shown under the conditions in Figure 1C. Bars are means of three independent counts for at least 50 cells; error bars are SEM. The symbol *** indicates significantly different from WT cells; $p < 0.001$.

(E) LC3 I and II levels following infection with indicated strains for 4 hr at MOI of 25 in WT or *Myd88*-deficient macrophages (KO); β-tubulin as loading control.

(F) As (E), but with cells from wild-type or *Trif* knockout mice.

(G and H) Shows effects of *Trif* knockout on LC3 puncta accumulation. Conditions and symbols as in (C) and (D).

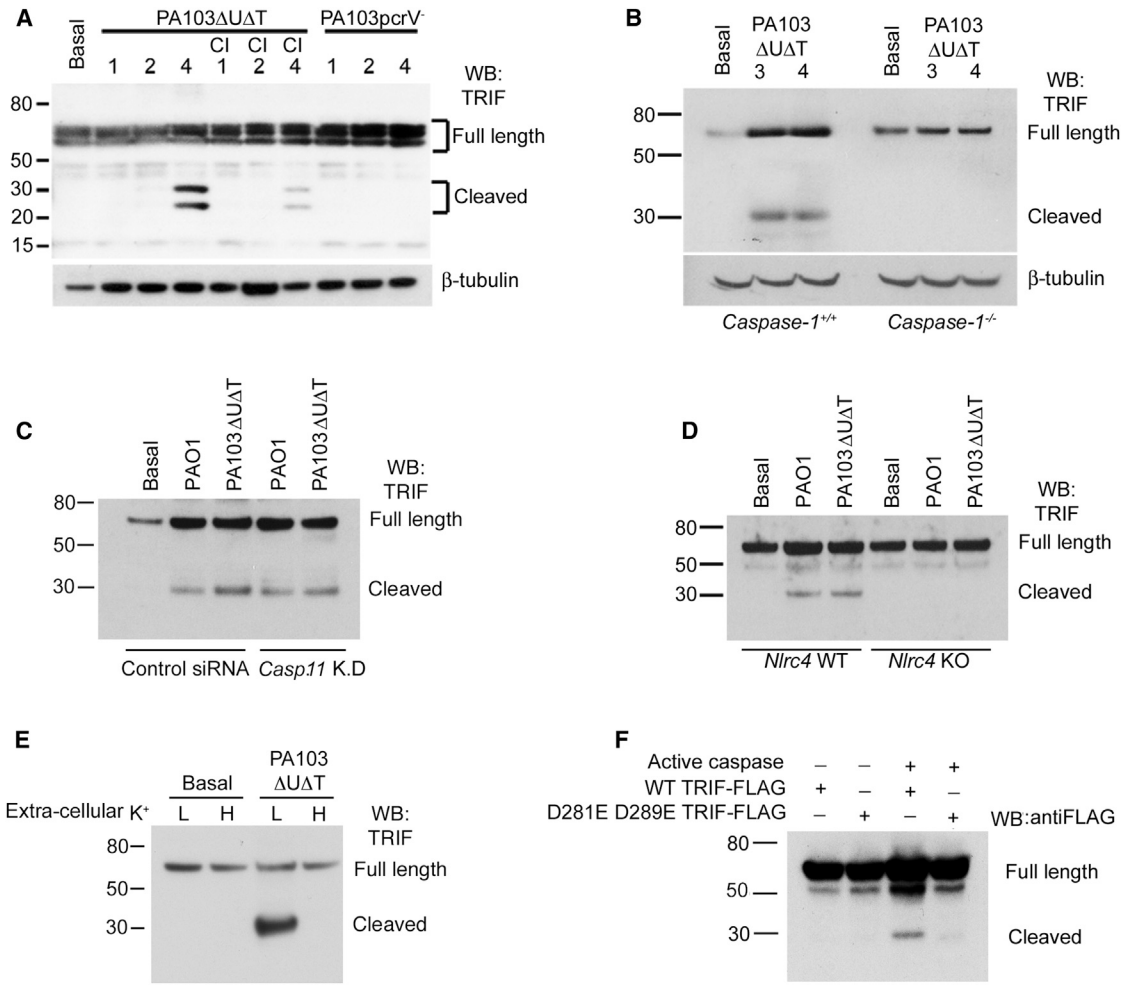

Figure 4. TRIF Is Cleaved by Caspase-1 following *P. aeruginosa* Activation of the Inflammasome

(A) Immunoblot (WB) for TRIF in BMDM that were uninfected (Basal) or infected with the *P. aeruginosa* strains shown for the indicated number of hours. Where shown, cells were treated with the caspase-1 inhibitor Z-YVAD-FMK (CI). Full-length and cleaved TRIF products are labeled. Molecular weight markers in kDa are shown to the left; β-tubulin is shown as a loading control (lower panel). Experiment repeated with the same results.

(B) As (A), but in BMDMs from WT (*Casp1*$^{+/+}$) or *Casp1* KO mice (*Casp1*$^{-/-}$).

(C) As (A), but cells transfected with Control siRNA or siRNA specific for *Casp11*, as shown.

(D) As (A), but in BMDMs from wild-type or *Nlrc4* knockout mice.

(E) As (A), but with cells in 5 mM K^+ (L) or 140 mM K^+ (H), as shown. Both experiments repeated with same results.

(F) Purified recombinant TRIF proteins as shown incubated with activated caspase-1, as shown, and analyzed by western blot. Molecular weight markers as in (B).

See also Figure S3.

reactive oxygen intermediates following infection of BMDMs with the T3SS-competent strain of *P. aeruginosa*, PA103ΔUΔT, compared to the T3SS-defective strain, PA103pcrV⁻. This showed that PA103ΔUΔT led to less phagocytosis and less production of reactive oxygen intermediates following infection compared to the PA103pcrV⁻ strain (Figure S5A). This is consistent with the reduced levels of type I IFNs resulting from inflammasome activation by the T3SS-competent strain and, hence, capsase-1 cleavage of TRIF. Importantly, adding β-IFN back to the BMDMs infected with the T3SS competent PA103ΔUΔT strain restored the level of phagocytosis and reactive oxygen production to the levels seen with the T3SS-defective PA103pcrV⁻ strain (Figure S5A). Thus, the defect in phagocytosis and production of reactive oxygen observed in the strain of *P. aeruginosa* that activates capsase-1 could be corrected by addition of a product normally produced via TRIF mediated signaling.

To establish that the reduction in these macrophage functions was due to caspase-1 degradation of TRIF, we tested the effect of removing TRIF or caspase-1 on phagocytosis and production of reactive oxygen. The ability of BMDMs from mice lacking TRIF to perform these functions was markedly reduced (Figure S5B). This inhibitory effect was reversed by the addition of β-IFN, demonstrating the importance of TRIF-mediated production of this cytokine in enhancing phagocytosis and production of reactive oxygen. Knock down of caspase-1 enhanced the ability of BMDMs to phagocytose and produce reactive oxygen following *P. aeruginosa* infection (Figure S5C). This enhancement in these

functions was similar to that seen following the addition of β-IFN to BMDMs infected with the inflammasome-activating *P. aeruginosa* strain PA103ΔUΔT (Figure S5A). Taken together, these results support the conclusion that capsase-1-mediated proteolysis of TRIF following *P. aeruginosa* infection of BMDMs leads to downregulation of IFN-β production and reduction in phagocytosis and reactive oxygen production.

To confirm that the cleavage of TRIF was responsible for the downregulation of phagocytosis and reactive oxygen production following caspase-1 activation, we examined these functions in BMDMs transfected with WT and noncleavable TRIF (D281E D289E TRIF). Compared to cells transfected with WT TRIF, BMDMs transfected with the D281E D289E TRIF had higher levels of phagocytosis and reactive oxygen production (Figure S5D). Again, we could increase the lower levels seen in cells expressing WT TRIF by addition of β-IFN. Thus, by preventing TRIF cleavage by caspase-1, we could augment the ability of BMDMs to phagocytose *E. coli* particles and produce reactive oxygen intermediates.

Next, we examined the net effect of these changes on the clearance of *P. aeruginosa* exposed to macrophages. Phagocytosis of the microbe will be followed by intracellular killing; we thus measured the numbers of viable intracellular bacteria present within macrophages as an indicator of the ability of these cells to clear the infection. Inhibiting caspase-1 reduced the numbers of viable intracellular bacteria; a similar reduction was achieved by pretreating the macrophages with type I IFN (Figure S5E). Absence of TRIF produced a rise in viable intracellular organisms that could be reversed by IFN (Figure S5F). Knockdown of caspase-1 had the same effect as caspase-1 inhibition (Figure S5G). These data are all consistent with TRIF-mediated type-I-IFN -dependent augmentation of macrophage killing being downregulated by caspase-1 action. To show that TRIF cleavage was important in this regard, we infected macrophages transfected with either WT or mutant D281E D289E TRIF. In the presence of the noncleavable TRIF, there was a reduction in viable intracellular bacteria. A similar reduction was achieved by treating the macrophages transfected with WT TRIF with type I IFN (Figure S5H).

Effects of Caspase-1 TRIF Cleavage on Infection with *P. aeruginosa* In Vivo

Next, we evaluated the effects of Caspase-1 TRIF cleavage on the cytokine responses and bacterial killing in an in vivo model of infection. We utilized an acute intraperitoneal model of *P. aeruginosa* infection in mice. Inhibition of caspase-1 with Z-YVAD-FMK led to reduced serum levels of IL-1β, as expected, with no reduction in TNF (Figure 6A). In cells harvested from the peritoneum 6 hr following infection (predominantly neutrophils), there was an increase in autophagy in animals treated with the caspase-1 inhibitor (Figure 6A) and a significant reduction in the numbers of viable bacteria recovered from the peritoneum (Figure 6A). These data suggest that the decreased IL-1β production and increased autophagy produced by caspase-1 inhibition result in increased bacterial clearance.

As a more direct test of the effect of preventing Caspase-1-mediated TRIF cleavage during infection, we set up the following animal model. We depleted intraperitoneal macrophages by instillation of liposomal clodronate (Figure 6B). We then reintroduced macrophages transfected with expression plasmids for either WT TRIF or the D281E D289E mutant. Autophagy within the introduced transfected macrophages was increased following infection in vivo (Figures 6C and 6D), and macrophages expressing the noncleavable TRIF mutant showed increased levels of autophagy compared to the WT protein. Interestingly, animals populated with macrophages expressing the noncleavable D281E D289E mutant TRIF had lower serum IL-1β levels compared to those populated with macrophages expressing WT TRIF; TNF levels were the same (Figure 6D). Expression of the noncleavable TRIF was also associated with significantly lower intraperitoneal protein concentrations and viable bacterial counts (Figure 6D). Thus, in this model, preventing TRIF cleavage results in increased autophagy following infection that is associated with reduced IL-1β production but decreased numbers of viable intraperitoneal bacteria. This suggests autophagy may well control NLRC4 inflammasome activation following *P. aeruginosa* infection, as has been found for NLRP3 inflammasome activation (Saitoh et al., 2008); this is considered further in the Discussion.

Effect of Caspase-1 TRIF Cleavage on Activation of the NLRP3 Inflammasome

Activation of the NLRP3 inflammasome has been shown to be triggered by mitochondrial damage (Nakahira et al., 2011); this is limited by autophagy of mitochondria—mitophagy. We reasoned that caspase-1-mediated inactivation of TRIF would limit mitophagy and thus could act to enhance NLRP3 activation, leading to greater capsase-1 activation and production of IL-1β. To test this hypothesis, we examined the effects of limiting TRIF cleavage by casapse-1 in BMDMs stimulated with LPS and ATP. Following LPS/ATP stimulation, we observed increased levels of capsase-1 p10 and secreted IL-1β, as expected, and cleavage of TRIF, as we have observed with inflammasome activation by *P. aeruginosa*. In the cells transfected with the D281E D289E TRIF mutant, we observed an increase in levels autophagy following LPS/ATP stimulation (Figure 7A). We also observed a marked reduction in inflammasome activation (Figure 7A) but no effect on TNF. Thus, a highly significant effect of the caspase-1-induced cleavage of TRIF is to inhibit ongoing autophagy that otherwise would severely limit the degree of inflammasome activation and resultant IL-1β produced.

We repeated this experiment but additionally downregulated autophagy using siRNA (Figure 7B). In cells in which autophagy was inhibited, the amount of secreted IL-1β and caspase-1 activation in the presence of WT TRIF was significantly increased compared to cells transfected with control siRNA (Figure 7B). This is consistent with autophagy downregulating the signals required to trigger NLRP3 inflammasome activation and secretion of IL-1β in response to LPS + ATP. In cells expressing the D281E D289E-mutant TRIF with inhibition of autophagy by *Lc3b* or *Atg5* knockdown, there was a reduction in secreted IL1-β, but this did not reach statistical significance compared to cells expressing WT TRIF (Figure 7B). This is consistent with the conclusion that the reduction in secreted IL-β in the presence of TRIF that cannot be cleaved by caspase-1 is as a result of an increase in autophagy and mitophagy that acts to attenuate the triggering of the NLRP3 inflammasome by LPS + ATP. Prevention of TRIF cleavage results in increased type I IFN production

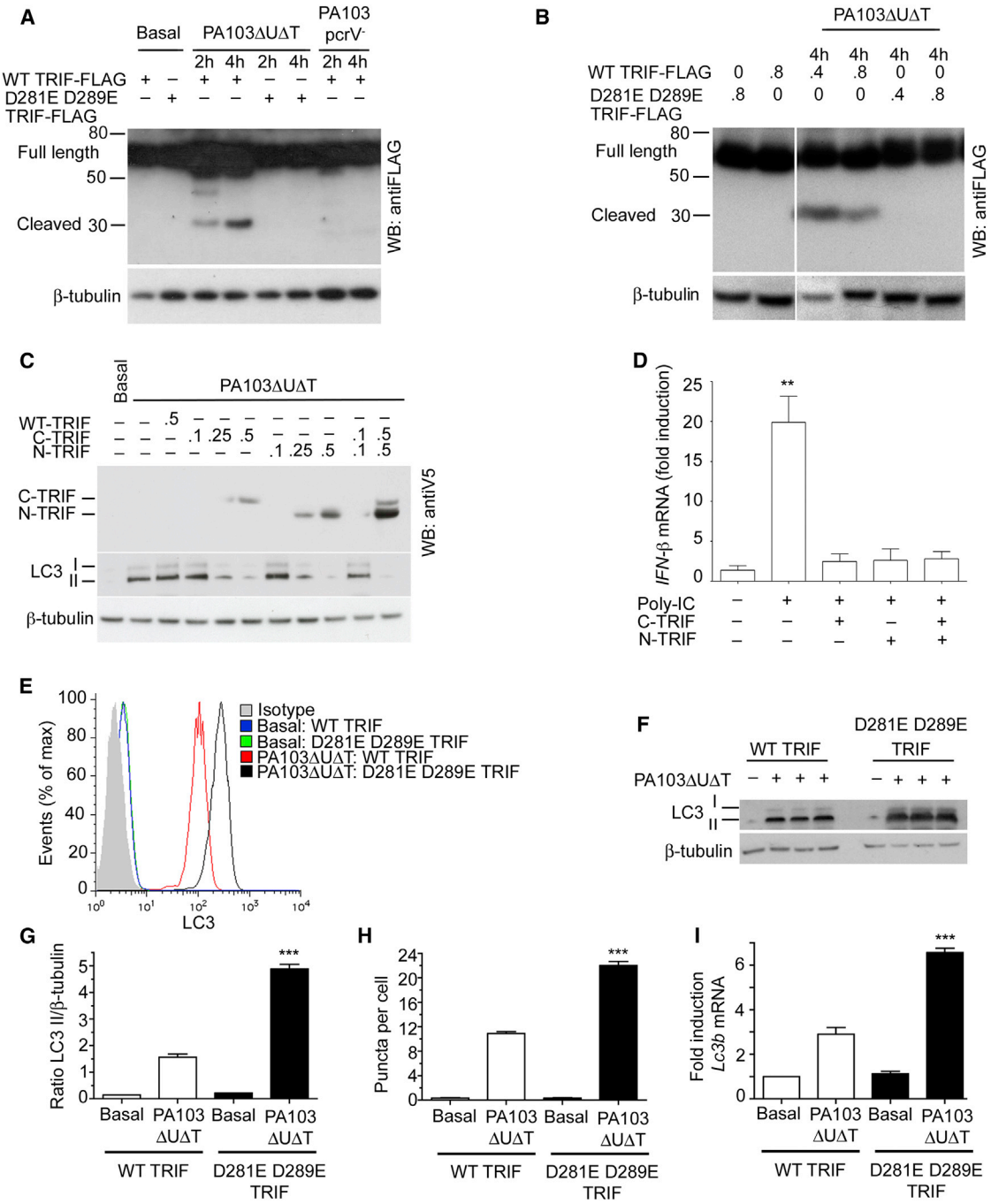

Figure 5. TRIF Cleavage by Caspase-1 Results in Downregulation of Autophagy

(A) Cells were transfected with plasmids as shown and then left uninfected (Basal) or infected for the indicated times with the *P. aeruginosa* strains indicated (MOI 25). Immunoblot was probed with anti-FLAG antibody. β-tubulin immunoblot is shown as loading control.

(B) Human THP-1 cells transfected with the indicated amounts of plasmids (in μg) were left uninfected or infected as shown (4 hr; MOI 25) and probed with antibody to FLAG. Experiment performed on two occasions with same results.

(C) BMDMs transfected with indicated amounts of TRIF expression plasmids (μg) and left uninfected (B) or infected as shown. Panel shows cell lysates blotted for V5 (epitope tag for TRIF) and LC3; β-tubulin shown as loading control.

(D) Levels of *Ifnb* mRNA assayed by RT-PCR following Polyl:C treatment (1 μg/ml for 5 hr) and transfection with TRIF constructs as shown. Columns are means of triplicates; error bars SEM. The symbol ** indicates significantly different from untreated ($p < 0.01$).

(E) Intracellular LC3 II levels assayed by flow cytometry in cells transfected with indicated plasmids and left uninfected (Basal) or infected as indicted (4 hr; MOI 25). Experiment performed on two occasions with same results.

(F) BMDMs transfected as in (A) and infected as shown (4 hr; MOI 25) and assayed for LC3 I and II levels by immunoblot.

(legend continued on next page)

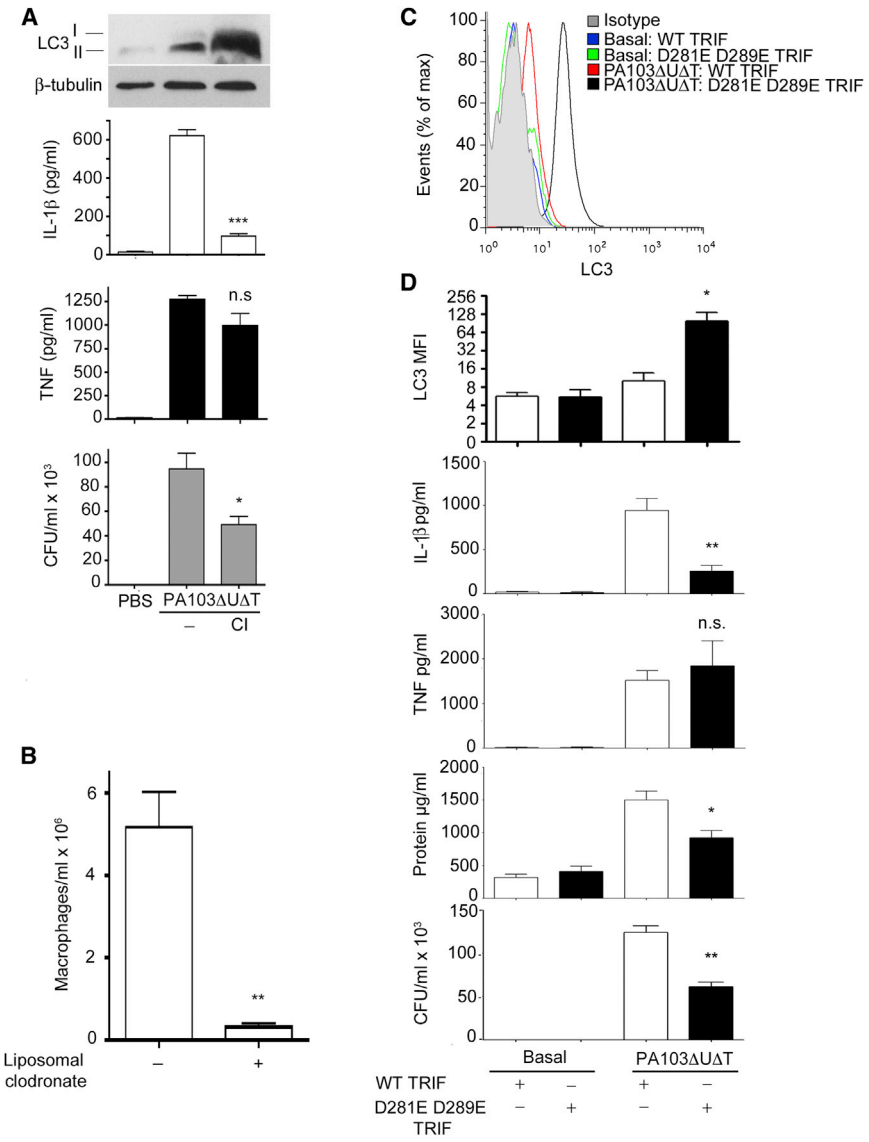

Figure 6. Role of TRIF Cleavage by Capsase-1 in an In Vivo Infection Model

(A) Panels show LC3 immunoblot with loading control of total cell extract from one representative animal, mean levels of serum IL-1β and TNF (n = 3, error bars are SEM), and recovered viable bacteria from the peritoneal cavity at 6 hr (n = 3; error bars SEM). Animals were pretreated with Z-YVAD-FMK (CI) as shown. The symbols * and *** are significant differences from untreated animals, $p < 0.05$ and $p < 0.001$, respectively.

(B) Peritoneal macrophage population in animals treated with liposomal clodronate as shown. Columns are means of three determinations; error bars are SEM. The symbols ** indicates significantly different from control ($p < 0.01$).

(C and D) Results from animals infected intraperitoneally following depletion of intraperitoneal macrophages and reconstitution with macrophages transfected as shown.

(C) Levels of intracellular LC3 II assayed by flow cytometry, gated on introduced macrophage populations, and transfected with constructs as shown. Representative plot from one animal.

(D) Panels show mean values of indicated measures from n = 3 animals; error bars are SEM. Values are of LC3 II mean fluorescence intensity (LC3 MFI), serum IL-1β and TNF, peritoneal protein concentration, and recovered viable bacterial colonies (CFU/ml × 10^3). Peritoneal macrophages were transfected with constructs as shown before repopulation of the peritoneal cavity. See also Figure S5.

in infection; this has been shown to suppress NLRP3 inflammasome activation principally through an IL-10-mediated downregulation of pro-IL-1β levels (Guarda et al., 2011) as well as an uncharacterized direct effect on the NLRP3 inflammasome that required at least 6 hr treatment. The suppressive effect of the noncleavable TRIF is evident after 4 hr of LPS/ATP, and we did not observe any changes in pro-IL-β or pro-caspase-1 levels in treated cells that had been transfected with the mutant D281E D289E noncleavable TRIF (Figure 7B). Thus, the observed effects of preventing TRIF cleavage on inhibiting NLRP3 activation by LPS/ATP would seem most likely mediated by the increased levels of autophagy rather than increased type I IFN production, although some contribution of type I IFN directly inhibiting NLRP3 inflammasome activation cannot be ruled out entirely. A corollary of the observed effects of preventing TRIF cleavage on NLRP3 activation is that in *Trif* knockout cells there should be an increase in NLRP3 activation by LPS/ATP because of the lack of autophagy. This is indeed the case, with a significant increase in IL-1β secretion and caspase-1 activation but no associated change in pro-IL-1β levels (Figure S6).

Finally, we extended these observations using the human macrophage cell line THP-1 (Figure 7C). In the presence of the mutant TRIF that cannot be cleaved by capsase-1, LPS + ATP produces less capsase-1 activation, less secreted IL-1β, and a greater amount of autophagy (Figure 7C).

DISCUSSION

In this study, we have shown that caspase-1 cleavage of TRIF results in a number of effects on immediate host defense to a

(G) LC3/β-tubulin ratio for three independent experiments under the indicated conditions. Columns show means; error bar is SEM. The symbol *** indicates significantly different from infected cells transfected with WT TRIF; $p < 0.001$.

(H) LC3 puncta in BMDMs transfected with indicated constructs and infected as shown (4 hr; MOI 25). The symbol *** indicates significantly different from infected cells transfected with WT TRIF; $p < 0.001$.

(I) Levels of *Lc3b* mRNA assayed with treatments as shown. See also Figure S4.

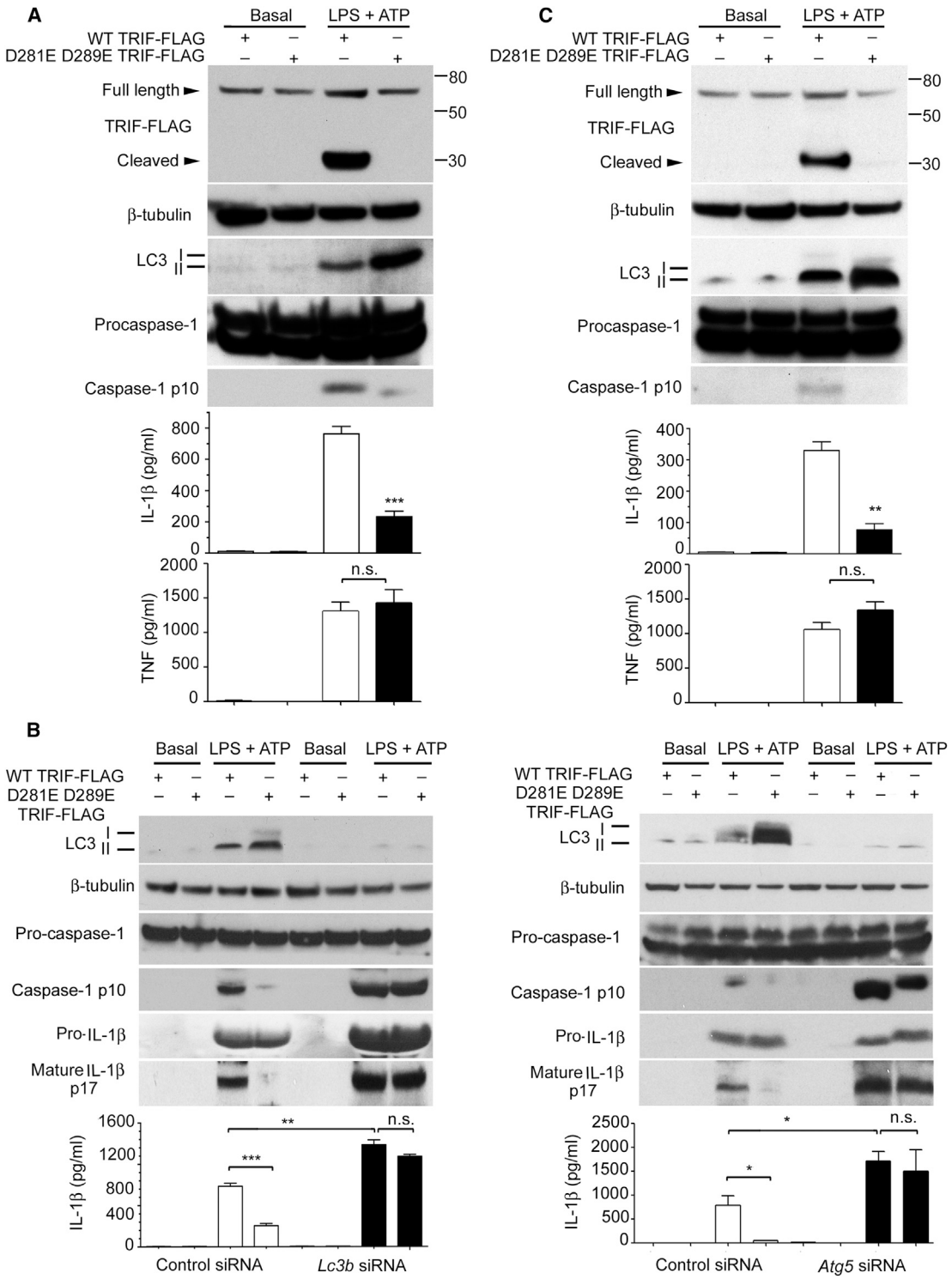

Figure 7. Prevention of TRIF Cleavage Attenuates NLRP3-Mediated Caspase 1 Activation and Production of Mature IL-1β

Cells were left untreated (Basal) or LPS (500 ng/ml) was added for 4 hr followed by 5 mM ATP for 20 min where indicated (LPS + ATP).

(A) BMDMs were transfected with plasmids as shown; panels show immunoblots of the indicated proteins. The bottom panel shows the levels of secreted IL-1β and TNF from the same cells as used in the immunoblotting with the treatments as indicated. Each column is mean of 3; error bars are SEM. Filled columns are results from cells transfected with the noncleavable TRIF and open columns from WT TRIF. The symbol *** indicates significant from WT; $p < 0.001$.

(B) BMDMs treated as indicated under the conditions described in (A). Cells were transfected with control siRNA or *Lc3b* siRNA (left panel) or control or *Atg5* siRNA (right panel). Statistical differences between bracketed columns are shown: **$p < 0.01$; ***$p < 0.001$.

(C) As (A), but in human THP-1 cells. All experiments repeated two to three times. See also Figure S6.

pathogen such as *P. aeruginosa*. On the one hand, the reduction in production of type I IFNs results in a diminution in macrophage phagocytosis and production of reactive oxygen. However, we also found that following in vivo infection, there was a reduction in production of IL-1β. This was associated with increased bacterial clearance, as has been found by others (Cohen and Prince, 2013). The reduction in IL-1β production following infection with *P. aeruginosa* under conditions where TRIF cleavage is blocked suggests that autophagy restrains NLRC4 inflammasome activation in this infection, in much the same way as has been shown for NLRP3 activation. We have gone on to explore this in depth and have found that autophagy does indeed inhibit NLRC4 inflammasome activation by *P. aeruginosa* (data not shown). The reduction in autophagy and mitophagy consequent to TRIF cleavage prevents these processes inhibiting caspase-1 activation. If TRIF were not cleaved in this way, the degree of activation of this inflammasome would be much less and production of IL-1β significantly reduced. The magnitude of this effect is large (Figure 7), and thus, we speculate that this is the principal evolutionary selection pressure that has maintained the cleavage site for caspase-1 within the TRIF protein. IL-1β is a key cytokine in innate immunity, and without cleavage of TRIF by caspase-1, the levels of active IL-1β following inflammasome activation would be much less. The overall effect of increased inflammasome activation consequent to TRIF cleavage varies depending on the specific infection involved. NLRC4 inflammasome activation is critical in host defense against *Klebsiella pneumonia* (Cai et al., 2012) and oral *Salmonella* infection in Balb/c mice (Franchi et al., 2012a), but it increases bacterial burden in a model of *P. aeruginosa* pneumonia (Cohen and Prince, 2013). Moreover, TRIF has been shown to be an important intermediate in triggering autophagy not only from TLR4 but also from TLR3 stimulation (Delgado et al., 2008). Thus, cleavage of TRIF may also play a role in limiting autophagy and enhancing inflammasome activation in infections that signal via TLR3, such as influenza. Additionally, a previous study with *Shigella flexneri*-infected macrophages suggested that capsase-1 activation limited autophagy (Suzuki et al., 2007). The data presented in the work described here suggest cleavage of TRIF would account for this effect.

TRIF has recently been shown to be an important intermediate in the induction of NLRP3 inflammasome activation by Gram-negative bacteria (Rathinam et al., 2012). Type I IFNs triggered by TLR4 via TRIF mediate the induction of capsase-11, a protease that can amplify caspase-1 activation by NLRP3. This has been shown to be of importance in infections caused by enterohemorrhagic *E. coli* and *Citrobacter rodentium* (Kayagaki et al., 2011), as well as other Gram-negative organisms (Aachoui et al., 2013; Broz et al., 2012). It does not seem to play a role in the activation of the NLRC4 inflammasome, the mechanism by which *P. aeruginosa* activates the inflammasome via its type III secretion apparatus. However, in organisms lacking a functional type III apparatus, the TLR4/TRIF/capsase-11 pathway can act to produce NLRP3 activation, albeit with much slower kinetics than the NLRC4-mediated effects (Rathinam et al., 2012). We show here, by specific knockdown of Caspase-11 using siRNA, that this protein does not play a role in the activation of the inflammasome by PA103ΔUΔT or in the cleavage of TRIF. From our results, we would predict that TRIF cleavage by caspase-1 would serve to downregulate activation of caspase-11 by attenuating the continued production of type I IFNs. The overall influence of TRIF cleavage in an infection will thus be dependent on potentially complex interactions between capsase-11 dependent and independent pathways.

Autophagy can downregulate the activation of the NLRP3 inflammasome by removal of damaged mitochondria (Nakahira et al., 2011). We describe here a reciprocal process by which inflammasome activation of caspase-1 acts to downregulate autophagy. Modulation of autophagy is thus a possible therapeutic target—either to limit its negative effects on inflammasome activation to augment host defense or to augment its action to limit excessive inflammation by caspase-1 and to enhance TRIF-mediated responses.

EXPERIMENTAL PROCEDURES

Materials

Rapamycin (50 μg/ml) and Z-YVAD-FMK (10 μg/ml) were from Enzo Lifesciences. Pepstatin (10 μg/ml), E64d (10 μg/ml), gentamicin, ATP, and LPS (*E. coli* O127:B8) were all from Sigma. IFN-β (Peprotech UK) was used at 10 ng/ml. PolyI:C (Invivogen) was used at 1 μg/ml for 5 hr.

Animals

Mice were maintained according to Institutional and National (UK Home Office) guidelines. C57/BL6 mice were obtained from Harlan UK. The following genetically modified mouse strains were used, all on the C57/BL6 background: *Tlr4*$^{-/-}$, (T. Mitchell, University of Glasgow), *Nlrc4*$^{-/-}$ (Mariathasan et al., 2004) from K. Fitzgerald (University of Massachusetts), *Casp1*$^{-/-}$ (Jackson Laboratories), *Vav-Atg7*$^{-/-}$ (Mortensen et al., 2010), *Trif*$^{-/-}$ (Yamamoto et al., 2003), and *Myd88*$^{-/-}$ (Yamamoto et al., 2003) (provided by D. Gray, University of Edinburgh).

Cells

Primary BMDMs were isolated as described from C57/BL6 mice (Celada et al., 1984). The human macrophage cell line THP-1 (gift of Dr. Damo Xu, University of Glasgow) was grown in RPMI 1640 medium supplemented with 10% fetal calf serum.

Bacteria

P. aeruginosa PA103ΔUΔT and PA103pcrV^{-} were kindly provided by Dara Frank. Bacterial strains were cultured in LB broth to mid-log phase (OD 0.4–0.6) immediately prior to use. Cells were washed twice in sterile PBS and used to infect cells at the indicated multiplicity of infection (MOI).

Cytokines

Cytokines in cell culture supernatants were measured by ELISA using the following kits: Murine IL-1β, R&D Systems (Cat No. DY401); murine TNF-α, eBioscience (Cat No. 88-7324-22); and human IL-1β (eBioscience). Murine IFN-β was from Peprotech (London, UK).

SiRNA and Transfection

Control siRNA and siRNAs to the indicated genes were all from Dharmacon (OnTarget plus SMART pool siRNA). Silencing constructs were introduced into cells using HiPerfect transfection reagent (QIAGEN), according to the manufacturer's instructions. Transfection of BMDMs was optimized using SiGLO Green transfection indicator (Dharmacon) and flow cytometry. We routinely achieved transfection efficiencies greater than 90% after 24–48 hr.

Plasmids and Transfection

N-terminal FLAG-tagged WT and D281E D289E TRIF constructs (Lei et al., 2011) in pcDNA3.1 were kindly provided by Dr. Lei. The N- and C-terminal constructs were made in pcDNA3.1 directional TOPO (Invitrogen) by PCR; sequences were verified by direct sequencing. Plasmids were transfected

into cells using Attractene (QIAGEN) according to the manufacturer's instructions. Cells were harvested at 24 hr after transfection.

qRT- PCR

Total RNA was isolated with an RNeasy Mini kit (QIAGEN) according to the manufacturer's instructions. cDNA was synthesized from DNaseI-treated RNA using Superscript II reverse transcriptase (Invitrogen) according to the manufacturer's instructions. Quantitative RT-PCR (qRT-PCR) was performed using power SYBR Green PCR master mix (Applied Biosystems) using the 7900HT fast system (Applied Biosystems) and primers, as described in the Supplemental Experimental Procedures. All determinations were performed in triplicate.

Immunoblot

The following antibodies were used: monoclonal anti-β-tubulin (Sigma-Aldrich), anti-Caspase-1 p10 (Santa Cruz Biotechnology), anti-LC3 (Novus Biologicals), anti-Atg5 (Novus Biologicals), anti-TRIF (Abcam), anti-FLAG (Sigma-Aldrich), anti caspase-11 (Santa Cruz), and anti V5 epitope (Sigma).

Immunofluorescence Microscopy

For immunofluorescence, LC3B was visualized using rabbit polyclonal LC3 (catalog number AP1802a, Abgent, USA). Sections were viewed using a Zeiss Axiovert S100 microscope using OpenLab software (PerkinElmer) or a LSM 510 Meta Confocal microscope (Carl Zeiss) using Meta 510 software. For quantification of LC3 puncta, image analysis was performed using Image J (NIH, Maryland). All results show values of mean number of puncta per cell; for each analysis at least 50 cells were analyzed.

LDH Release

Lactate dehydrogenase release determinations were performed using the Cytotox 96 cytotoxicity assay kit, catalog number G1781 (Promega, USA).

Flow Cytometry

Blocking of nonspecific Fc-mediated binding of antibodies to Fc receptors was performed using a rat anti-mouse CD16/CD32 antibody (BD Biosciences; 1ug/ml). Intracellular LC3B II was detected following the method described by Eng et al. (2010). Bacterial uptake was measured in cells using pHrodo *E.coli* BioParticles (Invitrogen; 1mg/ml for 2 hr at 37°C) prior to analysis by flow cytometry. Reactive oxygen intermediates were assayed using CellRox deep red reagent (Invitrogen; 5 μM for 30 min at 37°C) and flow cytometry. Cells were analyzed using a CyAn ADP (Beckman Coulter) or Facscalibur flow cytometer (BD). Flow cytometry data was analyzed with Flowjo Software (Tree Star Inc.).

Transmission Electron Microscopy

BMDM cells infected by PA for 4 hr were washed with Sorensen's Phosphate buffer and prefixed with 2% glutaraldehyde, followed by postfixation with 1% OsO_4 in 6.6 mM Sorensen's phosphate buffer. All pellets were dehydrated stepwise in a graded series of ethanol and embedded in araldite CY212. Ultrathin sections were double stained with uranyl acetate and lead citrate (all stains from Agar scientific). Sections were examined using a Tecnai transmission electron microscope (model number 943205018411, FEI Company; Czech Republic) equipped with Olympus digital camera (VELETA) at the Department of Pathology, Western Infirmary, Glasgow.

Infection Model

Peritoneal macrophages were depleted where indicated using clodronate liposomes (Foundation Clodronate Liposomes, Amsterdam). A total of 200 μl clodronate liposomes were injected 96 hr and 24 hr prior to infection. Depletion was confirmed by performing peritoneal lavage on animals injected with clodronate liposomes or PBS liposome controls and performing total cell counts and Romanowski staining after cytocentrifugation. BMDMs were stained with eFluor 450 proliferation dye (eBioscience) at a concentration of 10 μM according to the manufacturer's instructions. Where indicated, mice were injected intraperitoneally with 5×10^6 of eFluor-450-stained macrophages. In some experiments, animals were treated with Z-YVAD-FMK (0.1 mg/kg) intraperitoneally. One hour later, mice were injected with 10^7 cfu of PA103ΔUΔT or PBS intraperitoneally. After 6 hr, mice were culled by inhalation of CO_2. Peritoneal fluid was collected by injection and subsequent aspiration of 5 ml of cold PBS.

Neutrophils were enumerated by performing total cell counts and Romanowski staining after cytocentrifugation of peritoneal lavage fluid. Cells were then stained with Alexa Fluor 700 anti-CD11b (M1/70, Biolegend), PE anti-F4/80 (BM8, Biolegend), Alexa Fluor 647 anti-Ly-6G (1A8, Biolegend), or appropriate isotype controls. Following fixation and permeabilization, cells were then stained for LC3 as already described. Macrophages were selected on the basis of being CD11b+F4/80+Ly−6G−, and extrinsic macrophages were then identified on the basis of staining with eFluor 450.

Statistics

Comparison between groups at one time point was made using unpaired t test. A p value of < 0.05 was considered significant.

SUPPLEMENTAL INFORMATION

Supplemental Information includes six figures and Supplemental Experimental Procedures and can be found with this article online at http://dx.doi.org/10.1016/j.chom.2014.01.010.

ACKNOWLEDGMENTS

The study was supported by the Ministry of Higher Education and Scientific Research, Iraqi Cultural Attaché, London. M.S.J is a visiting scholar from the University of Technology, Applied Science School, Biotechnology Department, Baghdad, Iraq.

Received: October 24, 2013
Revised: January 8, 2014
Accepted: January 23, 2014
Published: February 12, 2014

REFERENCES

Aachoui, Y., Leaf, I.A., Hagar, J.A., Fontana, M.F., Campos, C.G., Zak, D.E., Tan, M.H., Cotter, P.A., Vance, R.E., Aderem, A., and Miao, E.A. (2013). Caspase-11 protects against bacteria that escape the vacuole. Science *339*, 975–978.

Arlehamn, C.S., Pétrilli, V., Gross, O., Tschopp, J., and Evans, T.J. (2010). The role of potassium in inflammasome activation by bacteria. J. Biol. Chem. *285*, 10508–10518.

Baehrecke, E.H. (2005). Autophagy: dual roles in life and death? Nat. Rev. Mol. Cell Biol. *6*, 505–510.

Bergsbaken, T., Fink, S.L., and Cookson, B.T. (2009). Pyroptosis: host cell death and inflammation. Nat. Rev. Microbiol. *7*, 99–109.

Broz, P., Ruby, T., Belhocine, K., Bouley, D.M., Kayagaki, N., Dixit, V.M., and Monack, D.M. (2012). Caspase-11 increases susceptibility to Salmonella infection in the absence of caspase-1. Nature *490*, 288–291.

Cai, S., Batra, S., Wakamatsu, N., Pacher, P., and Jeyaseelan, S. (2012). NLRC4 inflammasome-mediated production of IL-1β modulates mucosal immunity in the lung against gram-negative bacterial infection. J. Immunol. *188*, 5623–5635.

Celada, A., Gray, P.W., Rinderknecht, E., and Schreiber, R.D. (1984). Evidence for a gamma-interferon receptor that regulates macrophage tumoricidal activity. J. Exp. Med. *160*, 55–74.

Cohen, T.S., and Prince, A.S. (2013). Activation of inflammasome signaling mediates pathology of acute P. aeruginosa pneumonia. J. Clin. Invest. *123*, 1630–1637.

Delgado, M.A., Elmaoued, R.A., Davis, A.S., Kyei, G., and Deretic, V. (2008). Toll-like receptors control autophagy. EMBO J. *27*, 1110–1121.

Deretic, V., and Levine, B. (2009). Autophagy, immunity, and microbial adaptations. Cell Host Microbe *5*, 527–549.

Eng, K.E., Panas, M.D., Karlsson Hedestam, G.B., and McInerney, G.M. (2010). A novel quantitative flow cytometry-based assay for autophagy. Autophagy *6*, 634–641.

Franchi, L., Stoolman, J., Kanneganti, T.D., Verma, A., Ramphal, R., and Núñez, G. (2007). Critical role for Ipaf in *Pseudomonas aeruginosa*-induced caspase-1 activation. Eur. J. Immunol. *37*, 3030–3039.

Franchi, L., Eigenbrod, T., Muñoz-Planillo, R., and Nuñez, G. (2009). The inflammasome: a caspase-1-activation platform that regulates immune responses and disease pathogenesis. Nat. Immunol. *10*, 241–247.

Franchi, L., Kamada, N., Nakamura, Y., Burberry, A., Kuffa, P., Suzuki, S., Shaw, M.H., Kim, Y.G., and Núñez, G. (2012a). NLRC4-driven production of IL-1β discriminates between pathogenic and commensal bacteria and promotes host intestinal defense. Nat. Immunol. *13*, 449–456.

Franchi, L., Muñoz-Planillo, R., and Núñez, G. (2012b). Sensing and reacting to microbes through the inflammasomes. Nat. Immunol. *13*, 325–332.

Frank, D.W., Vallis, A., Wiener-Kronish, J.P., Roy-Burman, A., Spack, E.G., Mullaney, B.P., Megdoud, M., Marks, J.D., Fritz, R., and Sawa, T. (2002). Generation and characterization of a protective monoclonal antibody to *Pseudomonas aeruginosa* PcrV. J. Infect. Dis. *186*, 64–73.

Guarda, G., Braun, M., Staehli, F., Tardivel, A., Mattmann, C., Förster, I., Farlik, M., Decker, T., Du Pasquier, R.A., Romero, P., and Tschopp, J. (2011). Type I interferon inhibits interleukin-1 production and inflammasome activation. Immunity *34*, 213–223.

Kayagaki, N., Warming, S., Lamkanfi, M., Vande Walle, L., Louie, S., Dong, J., Newton, K., Qu, Y., Liu, J., Heldens, S., et al. (2011). Non-canonical inflammasome activation targets caspase-11. Nature *479*, 117–121.

Lei, X., Sun, Z., Liu, X., Jin, Q., He, B., and Wang, J. (2011). Cleavage of the adaptor protein TRIF by enterovirus 71 3C inhibits antiviral responses mediated by Toll-like receptor 3. J. Virol. *85*, 8811–8818.

Mariathasan, S., Newton, K., Monack, D.M., Vucic, D., French, D.M., Lee, W.P., Roose-Girma, M., Erickson, S., and Dixit, V.M. (2004). Differential activation of the inflammasome by caspase-1 adaptors ASC and Ipaf. Nature *430*, 213–218.

Martinon, F. (2012). Dangerous liaisons: mitochondrial DNA meets the NLRP3 inflammasome. Immunity *36*, 313–315.

Martinon, F., Mayor, A., and Tschopp, J. (2009). The inflammasomes: guardians of the body. Annu. Rev. Immunol. *27*, 229–265.

Miao, E.A., Ernst, R.K., Dors, M., Mao, D.P., and Aderem, A. (2008). *Pseudomonas aeruginosa* activates caspase 1 through Ipaf. Proc. Natl. Acad. Sci. USA *105*, 2562–2567.

Miao, E.A., Rajan, J.V., and Aderem, A. (2011). Caspase-1-induced pyroptotic cell death. Immunol. Rev. *243*, 206–214.

Mizushima, N., Yoshimori, T., and Levine, B. (2010). Methods in mammalian autophagy research. Cell *140*, 313–326.

Mortensen, M., Ferguson, D.J., Edelmann, M., Kessler, B., Morten, K.J., Komatsu, M., and Simon, A.K. (2010). Loss of autophagy in erythroid cells leads to defective removal of mitochondria and severe anemia in vivo. Proc. Natl. Acad. Sci. USA *107*, 832–837.

Nakahira, K., Haspel, J.A., Rathinam, V.A., Lee, S.J., Dolinay, T., Lam, H.C., Englert, J.A., Rabinovitch, M., Cernadas, M., Kim, H.P., et al. (2011). Autophagy proteins regulate innate immune responses by inhibiting the release of mitochondrial DNA mediated by the NALP3 inflammasome. Nat. Immunol. *12*, 222–230.

Orvedahl, A., and Levine, B. (2009). Eating the enemy within: autophagy in infectious diseases. Cell Death Differ. *16*, 57–69.

Rajan, J.V., Warren, S.E., Miao, E.A., and Aderem, A. (2010). Activation of the NLRP3 inflammasome by intracellular poly I:C. FEBS Lett. *584*, 4627–4632.

Rathinam, V.A., Vanaja, S.K., Waggoner, L., Sokolovska, A., Becker, C., Stuart, L.M., Leong, J.M., and Fitzgerald, K.A. (2012). TRIF licenses caspase-11-dependent NLRP3 inflammasome activation by gram-negative bacteria. Cell *150*, 606–619.

Rebsamen, M., Meylan, E., Curran, J., and Tschopp, J. (2008). The antiviral adaptor proteins Cardif and Trif are processed and inactivated by caspases. Cell Death Differ. *15*, 1804–1811.

Saitoh, T., Fujita, N., Jang, M.H., Uematsu, S., Yang, B.-G., Satoh, T., Omori, H., Noda, T., Yamamoto, N., Komatsu, M., et al. (2008). Loss of the autophagy protein Atg16L1 enhances endotoxin-induced IL-1beta production. Nature *456*, 264–268.

Shimada, K., Crother, T.R., Karlin, J., Dagvadorj, J., Chiba, N., Chen, S., Ramanujan, V.K., Wolf, A.J., Vergnes, L., Ojcius, D.M., et al. (2012). Oxidized mitochondrial DNA activates the NLRP3 inflammasome during apoptosis. Immunity *36*, 401–414.

Stromhaug, P.E., and Klionsky, D.J. (2001). Approaching the molecular mechanism of autophagy. Traffic *2*, 524–531.

Sutterwala, F.S., Mijares, L.A., Li, L., Ogura, Y., Kazmierczak, B.I., and Flavell, R.A. (2007). Immune recognition of *Pseudomonas aeruginosa* mediated by the IPAF/NLRC4 inflammasome. J. Exp. Med. *204*, 3235–3245.

Suzuki, T., Franchi, L., Toma, C., Ashida, H., Ogawa, M., Yoshikawa, Y., Mimuro, H., Inohara, N., Sasakawa, C., and Nuñez, G. (2007). Differential regulation of caspase-1 activation, pyroptosis, and autophagy via Ipaf and ASC in *Shigella*-infected macrophages. PLoS Pathog. *3*, e111.

Vallis, A.J., Finck-Barbançon, V., Yahr, T.L., and Frank, D.W. (1999). Biological effects of *Pseudomonas aeruginosa* type III-secreted proteins on CHO cells. Infect. Immun. *67*, 2040–2044.

Xu, Y., Jagannath, C., Liu, X.-D., Sharafkhaneh, A., Kolodziejska, K.E., and Eissa, N.T. (2007). Toll-like receptor 4 is a sensor for autophagy associated with innate immunity. Immunity *27*, 135–144.

Yamamoto, M., Sato, S., Mori, K., Hoshino, K., Takeuchi, O., Takeda, K., and Akira, S. (2002). Cutting edge: a novel Toll/IL-1 receptor domain-containing adapter that preferentially activates the IFN-beta promoter in the Toll-like receptor signaling. J. Immunol. *169*, 6668–6672.

Yamamoto, M., Sato, S., Hemmi, H., Hoshino, K., Kaisho, T., Sanjo, H., Takeuchi, O., Sugiyama, M., Okabe, M., Takeda, K., and Akira, S. (2003). Role of adaptor TRIF in the MyD88-independent toll-like receptor signaling pathway. Science *301*, 640–643.

Yu, H.B., and Finlay, B.B. (2008). The caspase-1 inflammasome: a pilot of innate immune responses. Cell Host Microbe *4*, 198–208.

Yuan, K., Huang, C., Fox, J., Laturnus, D., Carlson, E., Zhang, B., Yin, Q., Gao, H., and Wu, M. (2012). Autophagy plays an essential role in the clearance of *Pseudomonas aeruginosa* by alveolar macrophages. J. Cell Sci. *125*, 507–515.